Experimental observation of autosoliton propagation in a dispersion-managed system guided by nonlinear optical loop mirrors

Ashley Gray, Zhijian Huang, Yak W. A. Lee, Igor Y. Khrushchev, and Ian Bennion

Photonics Research Group, Department of Electronic Engineering, Aston University, Birmingham B4 7ET, UK

Received October 24, 2003

Observation of autosoliton propagation in a dispersion-managed optical transmission system controlled by in-line nonlinear fiber loop switches is reported for what is believed to be the first time. The system is based on a strong dispersion map with large amplifier spacing. Operation at transmission rates of 10 and 40 Gbits/s is demonstrated. © 2004 Optical Society of America

OCIS codes: 060.2330, 060.5530, 190.4360, 190.5530.

Ultralong-haul data transmission at high speeds over transoceanic distances represents a substantial technical challenge and usually requires the optical transmission system to support a stable optical carrier propagation. A variety of methods, including soliton transmission[1] and dispersion-managed (DM) soliton transmission,[2] have proved to be suitable for transoceanic signal propagation. These techniques provide, in principle, a solution to the problem of transmission at bit rates up to 40 Gbits/s. Speeds of 40 Gbits/s and above require additional efforts, such as a carefully designed dispersion map constructed from dispersion-shifted fiber.[3] In these advanced fiber links the dispersion map strength is relatively small. However, more than 90% of the installed fiber to date is standard single-mode fiber. Typically, the dispersion map strength in a standard-fiber system is in the range from 25 to 300. In such strong dispersion maps, neither the conventional soliton nor the DM soliton technique can provide stable carrier propagation over long distances.[4] As a result, the error-free transmission distance at 40 Gbits/s in standard fiber typically does not exceed 2000 km unless active regeneration techniques are employed.[5]

One way to extend the transmission distance is to utilize a passive regeneration method based on nonlinear intensity filtering in a nonlinear optical loop mirror (NOLM).[6–8] The technique has been known for some time; however, it has not been implemented to date for in-line data regeneration in long-haul systems.

Recent theoretical studies suggested that in-line NOLMs can provide a so-called autosoliton propagation regime in a DM fiber system.[9] An autosoliton can be described as an asymptotically stable solitary wave in a nonconservative medium, when, in addition to the equilibrium condition between nonlinearity and dispersion, there exists a balance among amplification, frequency-dependent damping, and nonlinear dissipation.[10] To our knowledge the existence of the NOLM-guided autosoliton regime has not yet been confirmed experimentally. In this Letter we present what is believed to be the first experimental observation of autosoliton propagation in a strongly DM system guided by in-line NOLMs and operating at speeds of 10 and 40 Gbits/s. In both cases, implementation of this autosoliton regime dramatically improved system performance.

The experimental setup is shown in Fig. 1. The carrier signal was provided by a mode-locked fiber ring laser (Ultrafast Optical Clock, Pritel) that was operated at a central wavelength of 1553.5 nm. The laser produced pulses of 3.5-ps duration at a repetition rate of 10 GHz. The signal was encoded with a pseudorandom bit pattern with a word length of $2^{31} - 1$ by means of a $LiNbO_3$ modulator. This 10-Gbit/s encoded signal was optically multiplexed to 40 Gbits/s.

The recirculating loop comprised two spans of standard single-mode fiber, 82 and 83 km long, and two slope-compensating fiber dispersion compensators. The average dispersion in the system was set to be slightly anomalous at approximately +0.003 ps/(nm km) at the operating wavelength. The corresponding dispersion map strength is 280. An electroabsorption modulator (EAM) was used in the receiver to demultiplex the signal from 40 to 10 Gbits/s.

The average signal power coupled into the recirculating loop was −9 dBm at a data speed of 10 Gbits/s

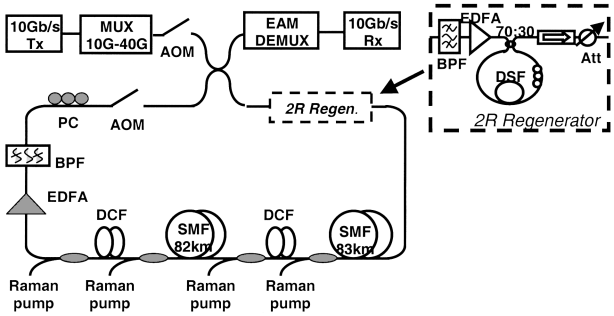

Fig. 1. Experimental setup: Tx, transmitter; MUX, multiplexer; AOM, acousto-optic modulator; DEMUX, demultiplexer; Rx, receiver; EDFA, erbium-doped fiber amplifier; BPF, bandpass filter; AH, attenuator; DSF, dispersion-shifted fiber; PC, polarization controller; DCF, dispersion-compensating fiber; SMF, single-mode fiber.

0146-9592/04/090926-03$15.00/0

and −3 dBm at 40 Gbits/s. The system was Raman amplified with the Raman pump waves counterpropagating with respect to the signal. A separate pump was used for each standard fiber and for each dispersion compensator. The Raman pump wavelength was 1455 nm.

We compared operation of the generic DM system as described above with that of an equivalent NOLM-guided system. For this purpose we added to the system a NOLM and a power amplifier to boost the power to the level required by the NOLM, as shown in Fig. 1. In addition, an attenuator was placed after the NOLM to balance the power in the system.

The NOLM used in this experiment comprised an asymmetric fiber coupler with a splitting ratio of 70:30 and 2.3 km of TrueWave fiber (OFS) with an anomalous dispersion of +2.8 ps/(nm km) at 1550 nm. The NOLM was placed at the beginning of the recirculating loop. The maximum transmission of the NOLM was reached at the input average power level of 1.3–1.4 W.

We investigated the signal dynamics in the system described above at data rates of 10 and 40 Gbits/s. At both speeds, the performance of the generic system was compared with that of the NOLM-guided system. The effect of the NOLM was immediately evident from the bit-error rate measurements. At the data transmission speed of 10 Gbits/s, the error-free transmission distance increased from 4300 km in the generic system to 11,000 km in the NOLM-guided system, as shown in Fig. 2(a). At 40 Gbits/s, there was a similar increase from 1000 km to more than 4000 km [Fig. 2(b)].

To study the NOLM-guided system in more detail we monitored the signal evolution in the spectral and temporal domains. The evolution of the 40-Gbit/s signal spectra in the generic and the NOLM-guided systems is presented in Fig. 3. In the generic system the signal spectrum experiences changes during the entire propagation time, as shown in Fig. 3(a). The signal gradually accumulates amplified spontaneous emission (ASE), which produces a narrow peak in the final spectrum, shown by the solid curve in Fig. 3(a). Multiple passes cause gradual narrowing of the ASE spectrum through the bandpass filters.

In the NOLM-guided system the spectrum evolves in a very different manner [Fig. 3(b)]. The spectral profile, well approximated by the sech^2 shape, is formed during the initial stage of propagation over several hundred kilometers. The spectrum does not change within the error-free propagation distance and remains remarkably stable well beyond this distance, up to 10,000 km and more.

The evolution of the temporal profile was characterized by use of a gated, background-free autocorrelator. Autocorrelation traces measured at several points in the generic system are shown in Fig. 4(a), and those taken in the NOLM-guided system are shown in Fig. 4(b). First, the pulse duration and shape were monitored as the signal propagated in the system. Additionally, we used the cross-correlated signal between adjacent pulses to estimate the timing jitter. For this purpose, autocorrelation traces were taken with the scanning range greater than the pulse-to-pulse period. As a result, each autocorrelation trace included a main peak and several additional peaks arising from the cross correlation between adjacent pulses. These additional peaks are broader than the main peak as a result of the timing jitter. The timing jitter was evaluated by using a procedure similar to that described in Ref. 11, as

$$\delta\tau \sim \frac{1}{4N}\sum_{k=1}^{N}\left(\frac{{\tau_k}^2 - {\tau_0}^2}{\ln 2}\right)^{1/2},$$

where τ_0 is the duration of the main peak in the autocorrelation trace and τ_k is the duration of the kth peak. A peak number k in the autocorrelation trace corresponds to the cross-correlated signal between pulses separated by k repetition periods. We therefore averaged the measurements over three pairs of peaks, thus improving the accuracy of the estimate.

In the generic system the pulse duration gradually increased because of nonzero average dispersion and reached 12 ps after 2500 km [Fig. 5(a)]. Although it was possible to balance the dispersion with greater precision and therefore to minimize pulse spreading, this configuration was found to show a reduced error-free transmission distance, and we chose not to study it any further. In the NOLM-guided system the pulse duration remained stable within the measurement accuracy and was measured as 3.6 ± 0.6 ps during transmission over more than 10,000 km. Notably, pulse spreading

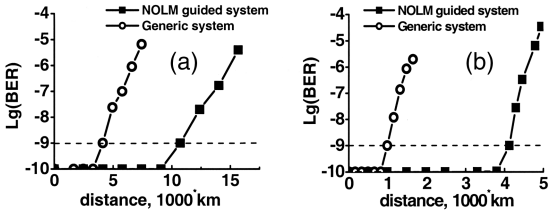

Fig. 2. Transmission performance at (a) 10 Gbits/s and (b) 40 Gbits/s. BER, bit-error rate.

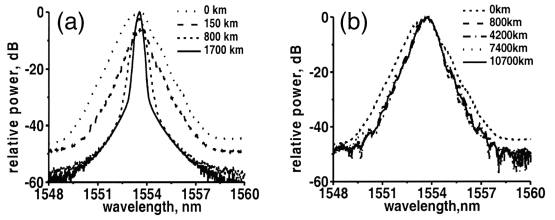

Fig. 3. Spectral evolution of the 40-Gbit/s signal in (a) the generic system and (b) in the NOLM-guided system.

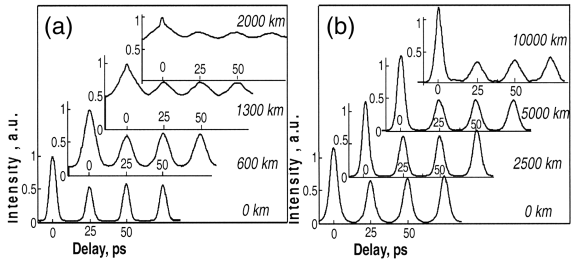

Fig. 4. Autocorrelation traces showing the 40-Gbit/s signal evolution in (a) the generic system and (b) the NOLM-guided system.

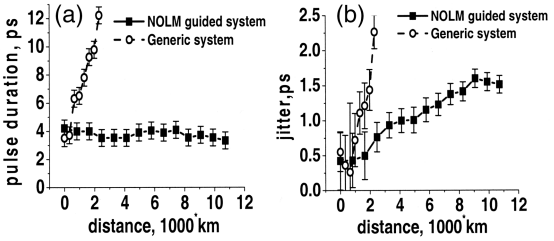

Fig. 5. Dynamics of (a) pulse duration and (b) jitter measured in the generic system and in the NOLM-guided system.

was virtually eliminated in the guided system in spite of the fact that the NOLM dispersion added to the average dispersion, making it greater than that in the generic system. The dispersive pulse broadening was compensated for by the self-phase modulation in the NOLM.

The timing jitter of the generic system increased almost linearly from <1 ps in the back-to-back signal to 2.1 ps after 2500 km [Fig. 5(b)]. A significant background appeared in the autocorrelation traces because of overlap of the dispersion-broadened adjacent pulses and an accumulation of ASE. The background increased significantly with distance. In the NOLM-guided system the timing jitter steadily increased, but the increase rate was lower than that in the generic system. The jitter accumulated after 10,000 km was 1.5 ps. Hence, the rate of the jitter increase was reduced from 1 fs/km in the generic system to approximately 0.1 fs/km in the guided system. We believe that the main mechanism responsible for the jitter improvement was the reduction of intersymbol interference as a result of the shorter average pulse duration in the guided system as well as the ASE suppression in this system.

The measurements confirmed the existence of autosolitons in the NOLM-guided system, in line with the earlier theoretical predictions.[9] The system parameters in the experiment were different from those in the simulation, and hence the results in the two studies cannot be compared directly. In spite of this, the main result in both cases was that a propagation regime exists in which the pulse duration, power, and spectrum, measured at a certain point in the system, remain stable over a virtually infinite distance. The NOLMs therefore act as $2R$ regenerators. The degradation of the data transmission performance in the NOLM-guided system is due mainly to the timing jitter increase. The measurements confirmed the constant increase of the timing jitter. In principle, it is possible to optimize the dispersion map by changing the map periodicity, symmetry, and strength[12] to reduce the accumulated timing jitter, which represents a potential for further improvement of the demonstrated method.

Autosoliton propagation in a dispersion-managed transmission system controlled by in-line NOLMs has been experimentally demonstrated. The in-line NOLM provides stabilization of the signal in the spectral and temporal domains as well as the ASE suppression. Improvement of the error-free propagation distance from 4300 to 11,000 km at 10 Gbits/s and from 1000 to 4000 km at 40 Gbits/s has been achieved.

The authors thank S. K. Turitsin for helpful discussions. A. Gray (e-mail graya@aston.ac.uk) acknowledges financial support from the UK Engineering and Physical Sciences Research Council and Indigo Photonics via a Co-operative Award in Science and Engineering studentship award.

References

1. L. F. Mollenauer, E. Lichtman, M. J. Neubelt, and G. T. Harvey, Electron. Lett. **29,** 910 (1993).
2. S. Penketh, P. Harper, S. B. Alleston, I. Bennion, and N. J. Doran, Opt. Lett. **24,** 802 (1999).
3. H. N. Ereifej, V. Grigoryan, and G. M. Carter, Electron. Lett. **37,** 1538 (2001).
4. E. Poutrina and G. P. Agrawal, Opt. Commun. **206,** 193 (2002).
5. K. Suzuki, H. Kubota, A. Sahara, and M. Nakazawa, Electron. Lett. **34,** 98 (1998).
6. N. J. Smith and N. J. Doran, J. Opt. Soc. Am. B **12,** 1117 (1995).
7. M. Meissner, M. Rosch, B. Schmauss, and G. Leuchs, IEEE Photon. Technol. Lett. **15,** 1297 (2003).
8. R. Ludwig, A. Sizmann, U. Feiste, C. Shubert, M. Kroh, C. M. Weinert, and H. G. Weber, in *European Conference on Optical Communication (ECOC) 2001* (Institute of Electrical and Electronics Engineers, Piscataway, N.J., 2001), paper Tu.B.2.7.
9. S. Boscolo, J. H. B. Nijhof, and S. K. Turitsyn, Opt. Lett. **25,** 1240 (2000).
10. V. S. Filho, F. Kh. Abdullaev, A. Gammal, and L. Tomio, Phys. Rev. A **63,** 053603 (2001).
11. J. Dörring, G. B. Tudury, A. Lenihan, G. M. Carter, and Y. J. Chen, Electron. Lett. **38,** 727 (2002).
12. S. K. Turitsyn, M. P. Fedoruk, T. S. Yang, and W. L. Kath, IEEE J. Quantum Electron. **36,** 290 (2000).